This is the accepted manuscript made available via CHORUS. The article has been published as:

Parity-time symmetry breaking in magnetic systems

Alexey Galda and Valerii M. Vinokur

Phys. Rev. B **94**, 020408 — Published 14 July 2016

DOI: 10.1103/PhysRevB.94.020408

Parity-Time Symmetry Breaking in Magnetic Systems

Alexey Galda[1] and Valerii M. Vinokur[1]

[1]*Materials Science Division, Argonne National Laboratory, 9700 S. Cass Avenue, Argonne, Illinois 60439, USA*

(Dated: May 25, 2016)

The understanding of out-of-equilibrium physics, especially dynamic instabilities and dynamic phase transitions, is one of the major challenges of contemporary science spanning the broadest wealth of research areas that range from quantum optics to living organisms. Focusing on non-equilibrium dynamics of an open dissipative spin system, we introduce a non-Hermitian Hamiltonian approach, in which non-Hermiticity reflects dissipation and deviation from equilibrium. The imaginary part of the proposed spin Hamiltonian describes the effects of Gilbert damping and applied Slonczewski spin-transfer torque. In the classical limit, our approach reproduces Landau–Lifshitz–Gilbert–Slonczewski dynamics of a large macrospin. We reveal the spin-transfer torque driven *parity-time* symmetry breaking phase transition corresponding to a transition from precessional to exponentially damped spin dynamics. Micromagnetic simulations for nanoscale ferromagnetic disks demonstrate the predicted effect. Our findings can pave the way to a general quantitative description of out-of-equilibrium phase transitions driven by spontaneous parity-time symmetry breaking.

I. INTRODUCTION

A seminal idea of parity-time ($\mathcal{PT}$)-symmetric quantum mechanics [1, 2], that has stated that the condition of Hermiticity in standard quantum mechanics required for physical observables and energy spectrum to be real can be replaced by less restrictive requirement of invariance under combined parity and time-reversal symmetry, triggered an explosive development of a new branch of science. The interpretation of $\mathcal{PT}$ symmetry as "balanced loss and gain" [3] connected $\mathcal{PT}$ symmetry-breaking to transitions between stationary and non-stationary dynamics and established its importance to understanding of the applied field-driven instabilities. Experiments on diverse variety of strongly correlated systems and phenomena including optics and photonics [4–10], superconductivity [11–13], Bose-Einstein condensates [14], nuclear magnetic resonance quantum systems [15], and coupled electronic and mechanical oscillators [16–18] revealed $\mathcal{PT}$ symmetry-breaking transitions driven by applied fields. These observations stimulated theoretical focus on far-from-equilibrium instabilities of many-body systems [12, 13, and 19] that are yet not thoroughly understood.

Here we demonstrate that non-Hermitian extension of classical Hamiltonian formalism provides quantitative description of dissipative dynamics and dynamic phase transitions in out-of-equilibrium systems. Focusing on the case of spin systems, we consider the zero-temperature spin dynamics under the action of basic non-conservative forces: phenomenological Gilbert damping [20] and Slonczewski spin-transfer torque [21] (STT). The latter serves as the most versatile way of directly manipulating magnetic textures by external currents. We propose a general complex spin Hamiltonian, in which Slonczewski STT emerges from an imaginary magnetic field. The $\mathcal{PT}$-symmetric version of the Hamiltonian is shown to exhibit a phase transition associated with inability of the system to sustain the balance between 'loss' and 'gain' above a certain threshold of external non-conservative field.

In the classical limit of a large spin, our formalism reproduces the standard Landau–Lifshitz–Gilbert–Slonczewski [20–22] (LLGS) equation of spin dynamics and predicts the $\mathcal{PT}$ symmetry-breaking phase transition between stationary (conservative) and dissipative (non-conservative) spin dynamics. In this Letter we focus on a single spin, yet our theory can be extended to coupled spin systems in higher dimensions. Moreover, as spin physics maps onto a wealth of strongly correlated systems and phenomena ranging from superconductivity to cold-atom and two-level systems, our results provide quantitative perspectives on the nature of phase transitions associated with $\mathcal{PT}$ symmetry-breaking in a broad class of far-from-equilibrium systems.

We introduce the non-Hermitian Hamiltonian for a single spin operator $\hat{\boldsymbol{S}}$:

$$\hat{\mathcal{H}} = \frac{E(\hat{\boldsymbol{S}}) + i\,\boldsymbol{j}\cdot\hat{\boldsymbol{S}}}{1 - i\alpha}\,, \tag{1}$$

where $E(\hat{\boldsymbol{S}})$ denotes the standard Hermitian spin Hamiltonian determined by the applied magnetic field $\boldsymbol{H}$ and magnetic anisotropy constants k_i in the x, y, z-directions: $E(\hat{\boldsymbol{S}}) = \sum_i k_i \hat{S}_i^2 + \gamma \boldsymbol{H}\cdot\hat{\boldsymbol{S}}$. A schematic system setup is shown in Fig. 1. The phenomenological constant $\alpha > 0$ in Eq. (1) describes damping; the imaginary field $i\boldsymbol{j}$ is responsible for the applied Slonczewski STT, with $\boldsymbol{j}S = \boldsymbol{e_p}(\hbar/2e)\eta J$ being the spin-angular momentum deposited per second in the direction $\boldsymbol{e_p}$ with spin-polarization $\eta = (J_\uparrow - J_\downarrow)/(J_\uparrow + J_\downarrow)$ of the incident current J; $\gamma = g\mu_B/\hbar$ is the absolute value of the gyromagnetic ratio; $g \simeq 2$, μ_B is the Bohr magneton; $\hbar$ is the Planck's constant, and e is the elementary charge. We conjecture that Eq. (1) serves as a fundamental generalization of the Hamiltonian description of both quantum and classical spin systems, which constitutes one of our core results. This form of the Hamiltonian proves extremely useful for the general understanding of STT-driven dissipative spin dynamics. In this work we focus primarily on the classical limit of spin dynamics, while the semiclassical limit of finite spin will be considered elsewhere.

Spin dynamics in the classical limit is conveniently obtained by studying expectation value of the Hamiltonian (1) with respect to SU(2) spin-coherent states [23, 24]: $|z\rangle = e^{z\hat{S}_+}|S, -S\rangle$, where $\hat{S}_\pm \equiv \hat{S}_x \pm i\hat{S}_y$, and $z \in \mathbb{C}$ is the standard stereographic projection of the spin direction on a unit

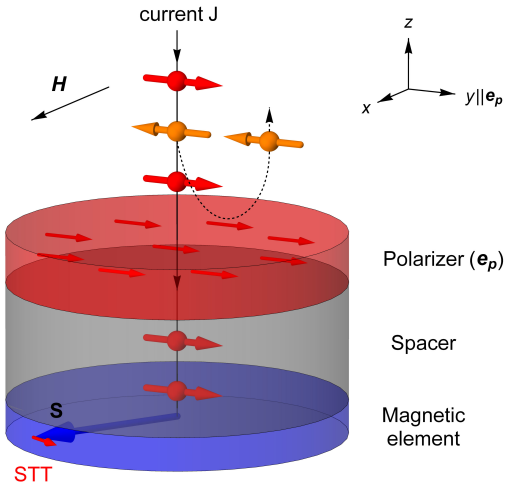

FIG. 1. Schematic representation of the system setup. Ferromagnetic cylinder (blue) is placed in magnetic field $\boldsymbol{H}$ applied along the x-axis, STT-inducing electric current J is polarized in the direction $\boldsymbol{e_p}$ along the y-axis. Spin-polarized current passes through a non-magnetic metallic spacer and induces torque (Slonczewski STT, shown by the small red arrow) on the total spin $\boldsymbol{S}$.

sphere, $z = (s_x + is_y)/(1 - s_z)$, with $s_i \equiv S_i/S$. Note that such parametrization of the phase space for a classical single spin system (i.e. in the limit $S \to \infty$) guarantees the invariance of the traditional equation of motion [24] under generalization to non-Hermitian Hamiltonians (see Supplemental Material):

$$\dot{z} = i\frac{(1+\bar{z}z)^2}{2S}\frac{\partial \mathcal{H}}{\partial \bar{z}}\,, \tag{2}$$

where z and $\bar{z}$ form a complex conjugate pair of stereographic projection coordinates, and

$$\mathcal{H}(z,\bar{z}) = \frac{\langle z|\hat{\mathcal{H}}|z\rangle}{\langle z|z\rangle} \tag{3}$$

is the expectation value of the Hamiltonian (1) in spin-coherent states (for a detailed review see, e.g., Ref. [25]). In this formulation, the eigenstates of $\hat{\mathcal{H}}$ correspond to the fixed points z_i of the equation of motion for $\mathcal{H}$, while the eigenvalues (i.e. energy values) are equal to $\mathcal{H}$ evaluated at the corresponding fixed points, $E_i = \mathcal{H}(z_i, \bar{z}_i)$.

Assuming a constant magnitude of the total spin, $\dot{S} = 0$, Eq. (2) reduces to the following equation of spin dynamics in the classical limit:

$$\dot{\boldsymbol{S}} = \nabla_S(\mathrm{Re}\mathcal{H}) \times \boldsymbol{S} + \frac{1}{S}\left[\nabla_S(\mathrm{Im}\mathcal{H}) \times \boldsymbol{S}\right] \times \boldsymbol{S}\,. \tag{4}$$

Here we refer to the real and imaginary parts of the Hamiltonian function $\mathcal{H}$ written in the spin $\boldsymbol{S}$-representation. For the non-Hermitian Hamiltonian (1), Eq. (4) reproduces the LLGS equation describing dissipative STT-driven dynamics of a macrospin:

$$\left(1+\alpha^2\right)\dot{\boldsymbol{S}} = \gamma \boldsymbol{H}_{\mathrm{eff}} \times \boldsymbol{S} + \frac{\alpha\gamma}{S}[\gamma \boldsymbol{H}_{\mathrm{eff}} \times \boldsymbol{S}] \times \boldsymbol{S} + \frac{1}{S}\,\boldsymbol{S} \times [\boldsymbol{S} \times \boldsymbol{j}] + \alpha\, \boldsymbol{S} \times \boldsymbol{j}\,, \tag{5}$$

$$\gamma \boldsymbol{H}_{\mathrm{eff}} = \nabla_S E(\boldsymbol{S})\,. \tag{6}$$

The first two terms in Eq. (5) describe the standard Landau–Lifshitz torque and dissipation, while the last two are responsible for the dissipative ('anti-damping') and conservative ('effective field') Slonczewski STT contributions, correspondingly, both of which appear naturally from the imaginary magnetic field term in the Hamiltonian (1).

$\mathcal{PT}$-SYMMETRIC HAMILTONIAN

Slonczewski STT turns the total spin-angular momentum, $\boldsymbol{S}$, in the direction of spin-current polarization, $\boldsymbol{e_p}$, without changing its magnitude. On the $\boldsymbol{S}$-sphere this can be represented by a vector field converging in the direction of $\boldsymbol{e_p}$ and originating from the antipodal point. It is the *imaginary* magnetic field $i\boldsymbol{j}$ that produces exactly the same effect on spin dynamics, according to Eq. (2). The action of STT is invariant under the simultaneous operations of time-reversal and reflection with respect to the direction $\boldsymbol{e_p}$, which is the underlying reason behind the inherent $\mathcal{PT}$ symmetry of certain STT-driven magnetic systems, including the one considered below.

Before turning to the $\mathcal{PT}$-symmetric form of Hamiltonian (1), we note that $\mathcal{PT}$-symmetric systems play an important role in the studies of non-equilibrium phenomena and provide a unique non-perturbative tool for examining the phase transition between stationary and non-stationary out-of-equilibrium dynamics. We show that despite being non-Hermitian, such systems can exhibit both of the above types of behavior, depending on the magnitude of the external non-conservative force. In the parametric regime of *unbroken* $\mathcal{PT}$ symmetry, systems exhibit physical properties seemingly equivalent [26] to those of Hermitian systems: real energy spectrum, existence of integrals of motion (see Supplemental Material), and, notably, the validity of the quantum Jarzynski equality [27]. However, in the regime of *broken* $\mathcal{PT}$ symmetry, one observes complex energy spectrum and non-conservative dynamics. Therefore, the 'true' transition between stationary and non-stationary dynamics can be identified as the $\mathcal{PT}$ symmetry-breaking phase transition.

Spin systems are generally subject to various non-linear magnetic fields including ones originating from shape, exchange, magnetocrystalline and magnetoelastic anisotropies. Restricting ourselves for simplicity to a second-order anisotropy term, we arrive at the following Hamiltonian for non-linear magnetic system with uniaxial anisotropy and applied Slonczewski STT:

$$\hat{\mathcal{H}}_{\mathcal{PT}} = \gamma H_0 \left(k_z \hat{S}_z^2 + h_x \hat{S}_x + i\beta \hat{S}_y\right)\,, \tag{7}$$

where the applied magnetic field h_x is measured in units of some characteristic magnetic field H_0, and β is a dimensionless STT parameter determining the relative to S amount of

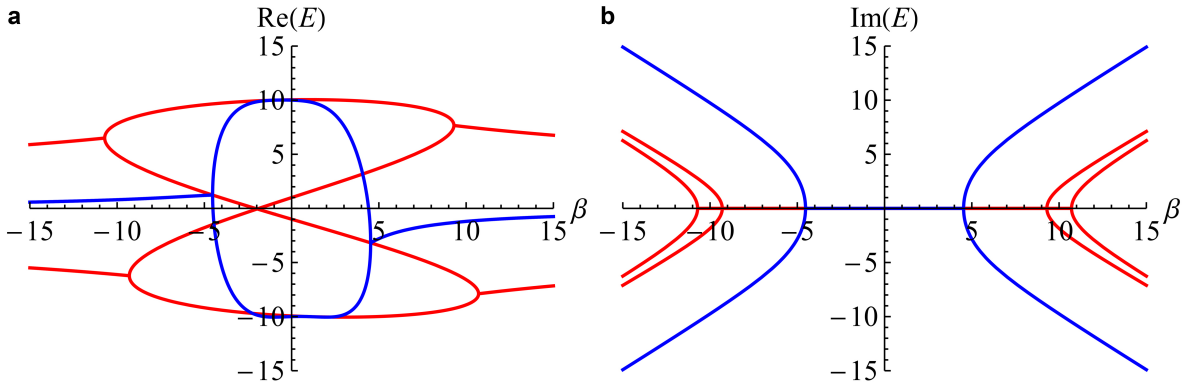

FIG. 2. Real **(a)** and imaginary **(b)** parts of energy spectrum of the Hamiltonian (7) as a function of the STT parameter β for $h_x = 1$ and $D = 20$. Blue and red lines correspond to the eigenvalues $E_{1,2}$ and E_{3-6}, respectively. The first $\mathcal{PT}$ symmetry-breaking transition occurs at $|\beta| = \beta_1 \approx 4.5$.

angular momentum transfered in time $\tau \equiv (\gamma H_0)^{-1}$ (characteristic timescale of the dynamics, used as a unit of dimensionless time in what follows). The Hamiltonian (7) modeling the dynamics of the free magnetic layer in a typical nanopillar device with fixed polarizer layer (see Fig. 1) is $\mathcal{PT}$-symmetric: it is invariant under simultaneous action of parity and time-reversal operators ($y \to -y$, $t \to -t$, $i \to -i$). Because the Hamiltonian $\hat{\mathcal{H}}_{\mathcal{PT}}$ commutes with an anti-linear operator $\mathcal{PT}$, its eigenvalues are guaranteed to appear in complex conjugate pairs. Notice that $\mathcal{PT}$-symmetric Hamiltonian (7) does not contain damping, which is assumed to be negligibly small, as is the case in many experimental systems.

CLASSICAL SPIN SYSTEM

In order to best illustrate the mechanism of $\mathcal{PT}$ symmetry-breaking, we focus on the classical limit, $S \to \infty$ and $k_z S \to D/2$, where D is the dimensionless uniaxial anisotropy constant. Formula (2) then yields the following equation of motion for the Hamiltonian (7):

$$\dot{z}(t) = -\frac{i(h_x+\beta)}{2}\left(z^2 - \frac{h_x-\beta}{h_x+\beta}\right) - iD\,z\frac{1-|z|^2}{1+|z|^2}\,, \qquad (8)$$

with up to six fixed points z_k, $k = 1, \ldots, 6$.

Shown in Fig. 2 are the real and imaginary parts of the energy spectrum E_{1-6} as functions of the STT amplitude β. It reveals that in a system with strong anisotropy, $D \gg 1$, $\mathcal{PT}$ symmetry breaking occurs in three separate transitions, with the first one at $|\beta| = \beta_1 = |h_x|\sqrt{[1+\sqrt{1+(2D/|h_x|)^2}\,]/2}$, which corresponds to the smallest amplitude of STT at which $\mathrm{Im}(E) \neq 0$. Therefore, $\mathcal{PT}$ symmetry is not broken in the entire phase space of initial spin directions simultaneously, at variance to the linear spin system with $D = 0$ (see Supplemental Material). Instead, the regions of broken and unbroken $\mathcal{PT}$ symmetry may coexist in the phase diagram of a non-linear spin system.

In what follows we consider a system described by the Hamiltonian (7) with $h_x = 1$ and $D = 20$. For all $|\beta| < \beta_1 \approx 4.5$, $\mathcal{PT}$ symmetry is unbroken and the character of spin (magnetization) dynamics is oscillatory in the entire phase diagram, i.e. for all possible initial conditions z. At $|\beta| = \beta_1$ the phase transition (first of the three, see Fig. 2) occurs sharply in a wide region around the easy plane, $|z| = 1$, i.e. near the equator of the unit $\boldsymbol{S}$-sphere, shown in gray in Fig. 3a, b in Cartesian and stereographic projection coordinates, correspondingly. It this region the nature of spin dynamics becomes fundamentally different – all spin trajectories follow the lines connecting the fixed points z_1 and z_2, where $z_{1,2} = -(Dh_x \pm i\sqrt{\beta^4 - \beta^2 h_x^2 - D^2 h_x^2})/(h_x+\beta)\beta$, and no closed trajectories are possible, see Fig. (3)b.

As $|\beta|$ is increased further, the region of broken $\mathcal{PT}$ symmetry expands until it eventually closes around the fixed point z_5 at $\beta_2 \approx 9.3$ (second bifurcation in Fig. 2) and, eventually, the last region of unbroken $\mathcal{PT}$ symmetry near z_3 disappears at $\beta_3 \approx 10.8$. The second and third phase transitions are less relevant experimentally as they occur in the vicinity of the least favorable spin directions (parallel and anti-parallel to the hard axis z) and at considerably higher applied currents.

The predicted transition from precessional dynamics (unbroken $\mathcal{PT}$ symmetry) to exponentially fast saturation in the direction $z_1(h_x, \beta)$ for any initial spin position around the easy plane (broken $\mathcal{PT}$ symmetry) occurs in the setup with mutually perpendicular applied magnetic field and Slonczewski STT. Such a transition in nanoscale magnetic structures can be used for STT- or magnetic field-controlled magnetization switching in spin valves and a variety of other experimental systems. This effect can further be used for direct measurements of the amplitude of the applied STT, which, unlike the applied current, can be hard to quantify experimentally.

NUMERICAL SIMULATIONS OF $\mathcal{PT}$ SYMMETRY BREAKING

Here we present the results of numerical simulations confirming the $\mathcal{PT}$ symmetry-breaking phase transition in the classical single spin system (7) by modeling magnetization dynamics of a ferromagnetic disk 100nm in diameter and

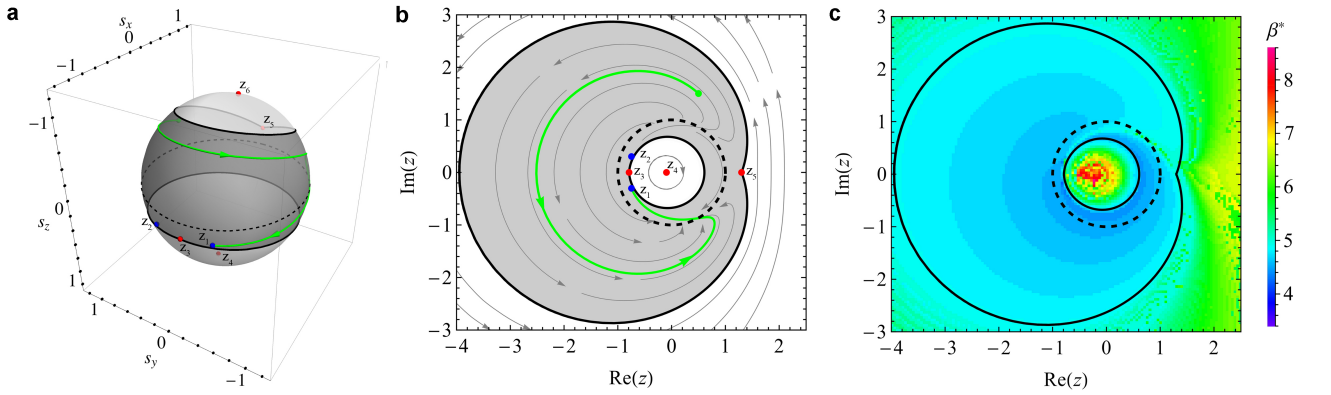

FIG. 3. **a, b**. Spin dynamics described by Eq. (8) with $h_x = 1$, $\beta = 4.7$, and $D = 20$. $\mathcal{PT}$ symmetry is broken in the shaded region around the easy plane $|z| = 1$ (dashed line), encompassing two fixed points, $z_{1,2}$ (blue dots), appearing as source and sink nodes. The green line depicts a typical non-oscillatory spin trajectory in the region of broken $\mathcal{PT}$ symmetry. Red dots represent the fixed points z_{3-6}. **c**. Results of micromagnetic simulations for β^* as a function of stereographic projection of the initial spin direction z. In the blue region, $4.6 \lesssim \beta^* \lesssim 4.8$, the $\mathcal{PT}$ symmetry is broken at all $|\beta| < \beta^*$, and the spin takes under 0.5ns to saturate in the direction of z_1, which is in full agreement with the analytical result.

$d = 5$nm thick, which is consistent with the anisotropy constant $D = 20$ in Eq. (8). We used the following typical permalloy material parameters: damping constant $\alpha = 0.01$, exchange constant $A_{\rm ex} = 13 \times 10^{-12}$J/m and saturation magnetization $M_{\rm sat} = 800 \times 10^3$A/m. The simulations were carried out using the open-source GPU-accelerated micromagnetic simulation program MuMax3 [28] based on the LLGS equation (5) discretized in space. We used a cubic discretization cell of 5nm in size, which is smaller than the exchange length in permalloy, $l_{\rm ex} = (2A_{\rm ex}/\mu_0 M_{\rm sat}^2)^{1/2} \approx 5.7$nm.

The permalloy disk was simulated in external magnetic field applied along the x-axis, $H_0 = 400$ Oe, which corresponds to the characteristic time $\tau \approx 0.14$ns. The STT was produced by applying electric current perpendicular to the disk in the z-direction with spin polarization $\eta = 0.7$ along $\boldsymbol{e_p} = \hat{y}$ (see Fig. 1) and current density β measured in dimensionless units of $2eH_0M_{\rm sat}d/\eta\hbar \approx 0.7\times10^8$A/cm^2. While such current density is comparable to typical switching current densities in STT-RAM devices [29, 30], its magnitude can be optimized for various practical applications by changing H_0 and adjusting the size, shape and material of the ferromagnetic element.

For all possible initial spin directions z, we calculated the critical amplitude of the applied STT, β^*, for which the character of spin dynamics changes from oscillatory (at $|\beta| < \beta^*$) to exponential saturation. Shown in Fig. 3c is the color map of β^* as a function of z in complex stereographic coordinates. The region shown in the shades of blue corresponds to the initial conditions z, for which the minimum values of β that would guarantee saturation of spin dynamics in the direction of z_1 in under 0.5ns are between 4.6 and 4.8. This is in full agreement with the region of broken $\mathcal{PT}$ symmetry at $\beta = 4.7$ calculated analytically, i.e. the shaded area in Fig. 3b (the outline is repeated in Fig. 3c for comparison). Outside of this region, a considerably larger magnitude of the applied STT is required to break $\mathcal{PT}$ symmetry.

The agreement between theoretical results and micromagnetic simulations is remarkable considering the non-zero Gilbert damping parameter ($\alpha = 0.01$) and non-linear effects (demagnetizing field, finite size/boundary effects, etc.) inherently present in the micromagnetic simulations but not included in the model Hamiltonian (7).

CONCLUSION

The presented non-Hermitian Hamiltonian formulation of dissipative non-equilibrium spin dynamics generalizes the previous result [31], where the classical Landau–Lifshitz equation was derived from a non-Hermitian Hamilton operator, to open STT-driven spin systems. The introduction of Slonczewski STT in the imaginary part of the Hamiltonian revealed the possibility of STT-driven $\mathcal{PT}$ symmetry-breaking phase transition. Micromagnetic simulations confirm the $\mathcal{PT}$ symmetry-breaking phenomenon in realistic mesoscopic magnetic systems and its robustness against weak dissipation, indicating high potential for impacting spin-based information technology. The way STT enters the complex Hamiltonian (1), i.e. as *imaginary* magnetic field, provides a unique tool for studying Lee-Yang zeros [32] in ferromagnetic Ising and Heisenberg models and, more generally, dynamics and thermodynamics in the complex plane of physical parameters. We envision further realizations of the $\mathcal{PT}$ symmetry-breaking phase transitions in diverse many-body condensed-matter systems and the expansion of practical implementations of the $\mathcal{PT}$ symmetry beyond the present realm of optics [33] and acoustics [34].

ACKNOWLEDGEMENTS

We thank Alex Kamenev for critical reading of the manuscript and valuable suggestions. The work is supported

by the U.S. Department of Energy, Office of Science, Materials Sciences and Engineering Division.

[1] C. M. Bender and S. Boettcher. Real spectra in non-Hermitian Hamiltonians having PT symmetry. *Phys. Rev. Lett.* **80**, 5243 (1998).

[2] C. M. Bender, S. Boettcher, and P. N. Meisinger. PT-Symmetric Quantum Mechanics. *Journ. Math. Phys.* **40**, 2201-2229 (1999).

[3] A. Ruschhaupt, F. Delgado, and J. G. Muga. Physical realization of PT-symmetric potential scattering in a planar slab waveguide. *J. Phys. A* **38**, L171 (2005).

[4] S. Klaiman, U. Günther, and N. Moiseev. Visualization of branch points in PT-symmetric waveguides. *Phys. Rev. Lett.* **101**, 080402 (2008).

[5] S. Longhi. Bloch oscillations in complex crystals with PT symmetry. *Phys. Rev. Lett.* **103**, 123601 (2009).

[6] S. Longhi. Optical realization of relativistic non-Hermitian quantum mechanics. *Phys. Rev. Lett.* **105**, 013903 (2010).

[7] H. Schomerus. Quantum noise and self-sustained radiation of PT-symmetric systems. *Phys. Rev. Lett.* **104**, 233601 (2010).

[8] H. Ramezani, T. Kottos, R. El-Ganainy, and D. N. Christodoulides. Unidirectional nonlinear PT-symmetric optical structures. *Phys. Rev. A* **82**, 043803 (2010).

[9] C. E. Rüter *et al.* Observation of paritytime symmetry in optics. *Nature Phys.* **6**, 192-195 (2010).

[10] J. Sheng, M. A. Miri, D. N. Christodoulides, and M. Xiao. PT-symmetric optical potentials in a coherent atomic medium. *Phys. Rev. A* **88**, 041803 (2013).

[11] J. Rubinstein, P. Sternberg, and Q. Ma. Bifurcation diagram and pattern formation of phase slip centers in superconducting wires driven with electric currents. *Phys. Rev. Lett.* **99**, 167003 (2007).

[12] J. Rubinstein, P. Sternberg, and K. Zumbrun. The resistive state in a superconducting wire: bifurcation from the normal state. *Arch. Ration. Mech. Anal.* **195**, 117 (2010).

[13] N. M. Chtchelkatchev, A. A. Golubov, T. I. Baturina, and V. M. Vinokur. Stimulation of the fluctuation superconductivity by PT symmetry. *Phys. Rev. Lett.* **109**, 150405 (2012).

[14] E. M. Graefe, H. J. Korsch, and A. E. Niederle. Mean-field dynamics of a non-Hermitian Bose-Hubbard dimer. *Phys. Rev. Lett.* **101**, 150408 (2008).

[15] C. Zheng, L. Hao, and G. L. Long. Observation of fast evolution in paritytime-symmetric system. *Phil. Trans. R. Soc. A* **371**, 20120053 (2013).

[16] C. M. Bender, B. K. Berntson, D. Parker, and E. Samuel. Observation of PT phase transition in a simple mechanical system. *Am. J. Phys.* **81**, 173 (2013).

[17] C. M. Bender *et al.* Twofold transition in PT-symmetric coupled oscillators. *Phys. Rev. A.* **88**, 062111 (2013).

[18] J. Schindler *et al.*. Experimental study of active LRC circuits with PT symmetries. *Phys. Rev. A* **84**, 040101(R) (2011).

[19] N. Poccia *et al.* Critical behavior at a dynamic vortex insulator-to-metal transition. *Science* **349**, 1202-1205 (2015).

[20] T. L. Gilbert. A phenomenological theory of damping in ferromagnetic materials. *IEEE Trans. Magn.* **40**, 3443 (2004).

[21] J. C. Slonczewski. Current-driven excitation of magnetic multilayers. *J. Magn. Magn. Matter*, **159**, L1-L7 (1996).

[22] L. D. Landau and E. M. Lifshitz. On the theory of the dispersion of magnetic permeability in ferromagnetic bodies. *Phys. Z. Sowjetunion* **8**, 101-114 (1935).

[23] E. H. Lieb. The classical limit of quantum spin systems. *Commun. Math. Phys.* **34**, 327-340 (1973).

[24] M. Stone, K.-S. Park, and A. Garg. The semiclassical propagator for spin coherent states. *Journ. Math. Phys.* **41**, 8025-8049 (2000).

[25] J. M. Radcliffe. Some properties of coherent spin states. *J. Phys. A* **4**, 313 (1971).

[26] A. Mostafazadeh. Exact PT-symmetry is equivalent to Hermiticity. *Journ. Math. Phys.* **36**, 7081 (2003).

[27] S. Deffner and A. Saxena. Jarzynski Equality in PT-Symmetric Quantum Mechanics. *Phys. Rev. Lett.* **114**, 150601 (2015).

[28] A. Vansteenkiste *et al.*. The design and verification of MuMax3. *AIP Advances* **4**, 107133 (2014).

[29] K. L. Wang, J. G. Alzate, and P. K. Amiri. Low-power non-volatile spintronic memory: STT-RAM and beyond. *J. Phys. D: Appl. Phys.* **46**, 074003 (2013).

[30] A. D. Kent, B. Özyilmaz, and E. Del Barco. Spin-transfer-induced precessional magnetization reversal. *Appl. Phys. Lett.* **84**, 3897 (2004).

[31] R. Wieser. Comparison of quantum and classical relaxation in spin dynamics. *Phys. Rev. Lett.* **110**, 147201 (2013).

[32] C. N. Yang and T. D. Lee. Statistical theory of equations of state and phase transitions. II. Lattice gas and Ising model. *Phys. Rev.* **87**, 410 (1952).

[33] B. Peng *et al.* Parity-time-symmetric whispering-gallery microcavities. *Nature Phys.* **10**, 394 (2014).

[34] R. Fleury, D. Sounas, and A. Alù. An invisible acoustic sensor based on parity-time symmetry. *Nature Commun.* **6**, 7413 (2015).